An Improved Two-Dimensional Numerical Modeling Method for E-Core Transformers

Anderson F. Hoke
A.B. Honors Thesis, June 2001
Advisor: Charles R. Sullivan

Thayer School of Engineering, 8000 Cummings Hall
Dartmouth College, Hanover, NH 03755-8000

Abstract: *Existing three-dimensional numerical modeling techniques for E-core transformers are accurate but require prohibitive amounts of simulation time. Hence, two-dimensional models are often used, but they are frequently inaccurate. We propose a new 2D modeling method that adds an extended flux return path to the model of the transformer section perpendicular to the core. Averaged (subject to appropriate weighting) with a section parallel to the core modified to have the same reluctance as the 3D model, the results from our model for total magnetic energy and magnetic energy in the windings are within 0.2-5.6% error relative to the 3D model in 15/16 cases.*

I. Introduction

Problems with Existing Methods:

There currently does not exist a reliable method for computer modeling of E-core transformers, such as the one in shown Figure 1, in two dimensions. Three-dimensional modeling of such transformers using finite element analysis (FEA) or other numerical methods is highly accurate and is not extremely difficult, but it is very time-consuming, even on fast computers. In addition to large time requirements, 3D models require very large amounts of free memory to provide accurate solutions. Using Ansoft's Maxwell 3D Field Simulator software on an MS Windows 2000 platform running on a Pentium 4 processor, a 3D model of the transformer in Figure 1 requires 289 seconds and 181 Mb of memory to arrive at a value of the total magnetic energy accurate to 2%, according to the software's error estimation algorithm. On the other hand, on the same machine, a 2D simulation of the same transformer to 1% accuracy requires 1 second and 21 Mb of memory. Either simulation may be sufficient for an engineer desiring to model one transformer a single time if he has a similar computer with plenty of disk space and is not in a hurry. However, when using the model iteratively to optimize some characteristic of a transformer, it is not practical to use a 3D simulation. For these reasons, in practice 2D numerical modeling is commonly used.

Although two-dimensional numerical modeling techniques are widely used, they fail to account for important 3D effects. The most basic 2D simulation involves modeling a cross-section parallel to the transformer core's longer sides, as shown in Figure 2a. This model can then be simulated by FEA assuming axial symmetry about the center of the transformer core. However, this approach ignores all 3D effects, which have been shown to be significant [1], [2]. The most straightforward approach to accounting for 3D effects would be to also model a section perpendicular to the plane of

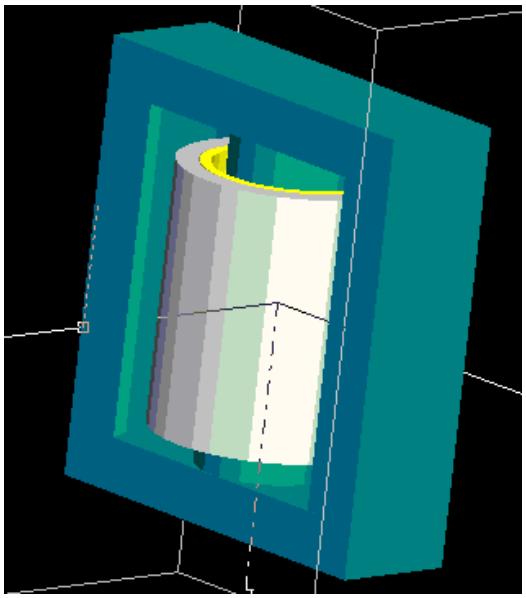

Figure 1: An E-core transformer.

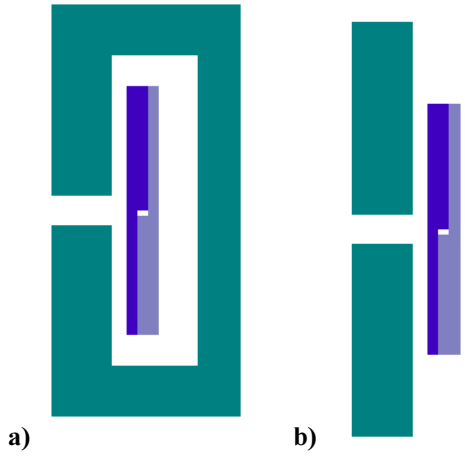

Figure 2: a) The section parallel to the core. b) The section perpendicular to the core

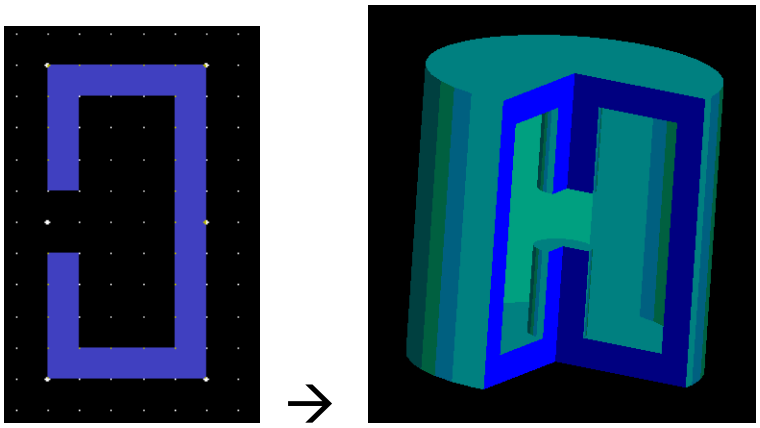

Figure 3: FEA uses axial symmetry, as shown here.

Figure 4: A 2D model modified to have the same reluctance as the 3Dmodel.

the core, as shown in Figure 2b and proposed in [3]. This method works well for the specific situation tested in [3] due to the way the particular winding shape used reduces the effect of current in one plane causing fields in the perpendicular plane. However, it fails in many other situations, as will be demonstrated in a later section of this paper.

A further inaccuracy in existing 2D modeling methods stems from the assumption of rotational symmetry about the center of the transformer. As shown in Figure 3, when modeling a section parallel to the core, the actual shape that the 2D FEA tool simulates is one with cylindrical symmetry, which consequently increases the cross-sectional area of the outer legs. As in [4], this effect can be accounted for by modifying the 2D model to have the same total reluctance as the 3D model (Figure 4). This modification is helpful in certain situations but once again does not accurately model the field in all areas, especially in the crucial area of the windings in the plane perpendicular to the core.

Overview of the Proposed New Method:

This paper proposes a new method of modeling E-core transformers in two dimensions using a weighted average of results from two modified, mutually perpendicular sections. We want to somehow create two 2D models that will simulate the behavior in the two sections shown in Figure 5. To model the section parallel to the core, we can use the section modified to have equal reluctance to the 3D model when simulated axisymmetrically, as described above and shown in Figure 4. The other section will be a modified version of the section perpendicular to the core. In order to create it, we recognize that the major difference between the 3D and 2D models of this section is the lack of availability of an outer flux path in the 2D model, since in the 3D model, magnetic flux is free to return though the core in another plane. Therefore our 2D model of this section should include a flux return path. However, the parallel, equal reluctance 2D model will not provide accurate results because of the proximity of the outer flux path to the windings. Instead, we use the model shown in Figure 6, which has an extended outer flux return path and is still designed to have the same reluctance as the 3D model. This path allows flux to return through core material without directing it

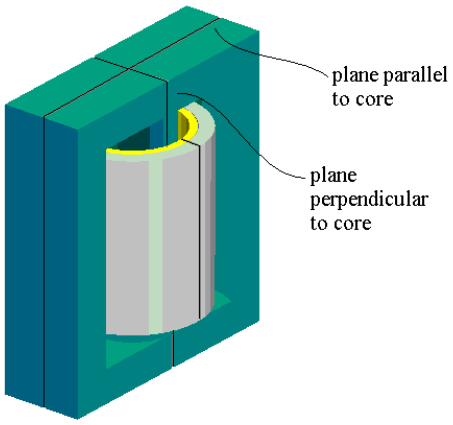

Figure 5: The two planes we hope to simulate.

Figure 6: The new extended path model for simulation of the plane perpendicular to the core.

unrealistically close the winding. A weighted average of results from each of these two models (Figures 4 and 6) can then be used to approximate values of interest. The weighting factor is based on an estimate of the relative amounts of the 3D model estimated to be effected by conditions similar to each section. The methods of mathematical determination of the weighting factor and of the two section geometries appear in Section II of this paper.

The Test Cases:

Before presenting a detailed description of our modeling method, we will summarize the various situations we hope to model and the values we hope to calculate for each. Varying only the presence and location of gaps in the basic E-core transformer, four different configurations are possible: the basic transformer with no gaps, the center gapped transformer, the outer gapped transformer, and the transformer with gaps in all three legs (Figure 7). In this paper the only winding setup that is considered is that of two concentric windings around the center post. In this case there are two distinct winding excitations: one in which the current in the two wires is parallel (magnetizing excitation), and one in which the two currents run antiparallel (leakage excitation).

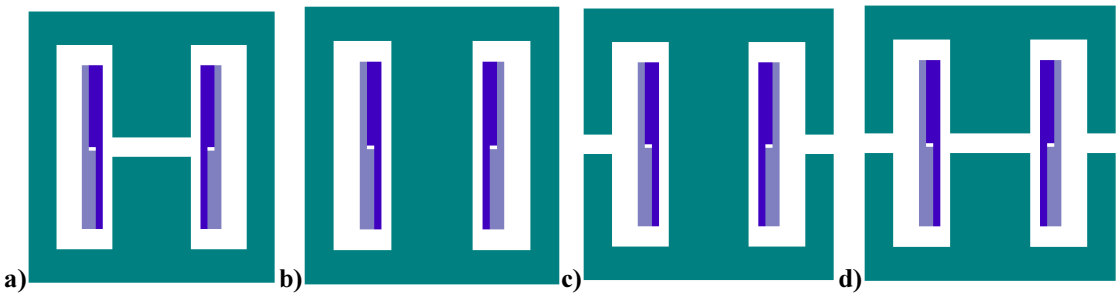

Figure 7: a) Center gapped core b) Gapless core c) Outer gapped core d) All gapped core.

For each of these four gap configurations and each of the two winding excitations we hope to compute values for two interesting volume integrals. The first is the total of B*H for the system, which is related to the total energy and to the inductance:

$$\textbf{total magnetic energy} = \frac{1}{2}\int_{otal} B \bullet H dv$$

The second is the integral of B*H inside the two windings, which is related to eddy current loss in the windings:

$$\textbf{magnetic energy in the winding region} = \frac{1}{2}\int_{windings} B \bullet H dv$$

A summary of these sixteen situations to be tested is shown in Table I. Each of the 2D modeling techniques, including those previously developed by others, will be tested in each situation. They will then be compared to the 3D FEA solution to determine their accuracy.

	magnetizing excitation		leakage excitation	
	total energy	winding energy	total energy	winding energy
no gap				
center gap				
outer gap				
all gap				

Table I: The sixteen situations for which the various 2D methods are to be evaluated

II. Detailed Description of New Method

The Four Sections and the Two Combined Sections:

First we will introduce some abbreviations for the various transformer sections that we will be modeling. The basic section parallel to the core is referred to herein as the || section. For the other basic section, perpendicular to the core, the abbreviation T is used. The first modified section, whose only modification is to trim the outer leg to give it a reluctance equal to that of the 3D model, is referred to as ER, for equal reluctance. The ER section is intended to model the section of the 3D model that is parallel to the core. The second modified section, which contains an imaginary extended flux return path and is also designed to have the same reluctance as the real transformer, is abbreviated XP, for extended path. It is intended to model the section perpendicular to the core.

Also useful in this discussion are two weighted combinations of the four sections. The combination put forth in [3] and [5] is an average of the section parallel to the core (||)with the section perpendicular to the core (T). It will be abbreviated ||T. The other combination is the one proposed herein and predicted to be most accurate. It consists of a weighted average of the equal reluctance section (ER) and the section containing the extended flux path (XP), and will be referred to as the ERXP model.

Determination of the Weighting Factor:

When calculating some value using one of the combined models, it is a reasonable initial approximation to give equal weighting to each of the two sections involved. In this case one would simply average the values determined from each section individually. For some specific geometries, such as the one used in [6], this would indeed be the best approximation to the actual 3D value. However, this is not necessarily the case for all geometries. Consider a view from above the transformer on which we have been focusing (as if looking down though the middle of the winding, as in Figure 8). Presumably, the part of the winding that is covered by the top piece of the core in this view is in a situation similar to that modeled by the ER section, and the part of the winding that is visible outside the core in this view is best modeled by the XP section. While a decent approximation to the relative areas of the two parts of the winding can be obtained by averaging the two angles labeled Θ_1 and Θ_2 in Figure 8, experimentation actually shows that better results are obtained when the exact areas of the two winding regions are computed. Therefore we have

$$w = A1 \Big/ (A1 + A2)$$

Hence, we define

$$\|T \equiv w*T + (1-w)*\|$$

and

$$ERXP \equiv w*XP + (1-w)*ER.$$

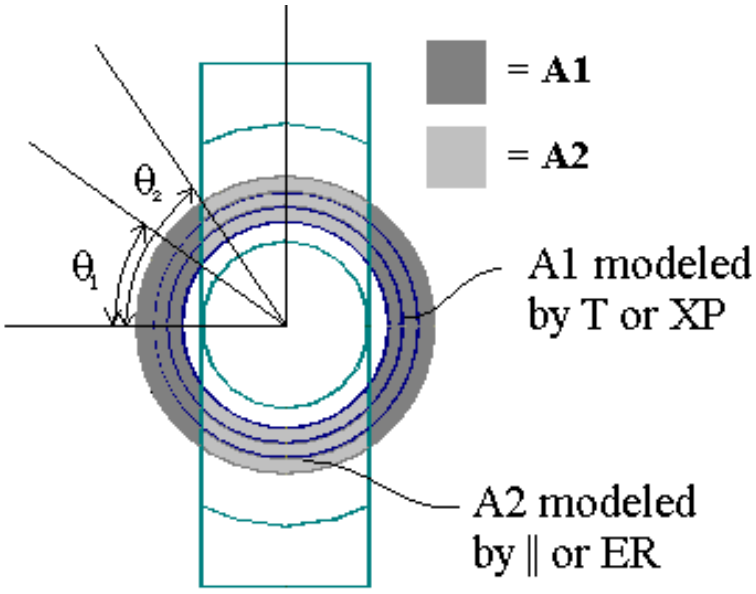

Figure 8: Determining the weighting factor.

Finding the Actual Core Reluctance for Use in Drawing ER and XP Models:

The accuracy of the calculation of the reluctance of the core turns out to be a major determining factor in the accuracy of the ER (equal reluctance) and XP (extended path) models. In transformer cores with gapped outer legs, finding the total reluctance requires the estimation of several fringing reluctances. The reluctance of a piece of core of relative permeability μ_R, length l, and cross sectional area A (as in Figure 9) is

(1) $$\Re = \frac{l}{\mu_0 \mu_R A},$$

where μ_0 is the permeability of free space. Therefore, a first approximation to the reluctance of an air gap of length l_{gap} and facing core area A is

(2) $$\Re_{gap} \approx \frac{l_{gap}}{\mu_0 A}.$$

However, this does not account for any of the significant amount of flux that exits the core some distance from the gap and fringes around it. In [7], a formula for the fringing reluctance is developed for 2D translationally symmetric transformers. Modeling a transformer cross section under translational symmetry treats the cross section shape as uniform along the direction perpendicular to the section, out to positive and negative infinity. Hence, all values derived are for a unit depth of the transformer, where the depth dimension is closest to perpendicular to the page in Figure 9. The formula given in [7] for the reluctance across a gap of length l_{gap} in a core leg of width w and length l (as shown in Figure 9) is

$$\Re_{gap,fringing} = \frac{1}{\mu_0 \left[\frac{w}{l_{gap}} + \frac{2}{\pi} \left(1 + \ln \frac{\pi l}{2 l_{gap}} \right) \right]}.$$

This formula represents the parallel combination of the reluctance of the path directly across the gap

$$\Re_{direct} = \frac{l_{gap}}{\mu_0 w}$$

and the fringing reluctance

$$\Re_{fringing,2D} = \frac{\pi}{2\mu_0 \left(1 + \ln \frac{\pi l}{2 l_{gap}} \right)}$$

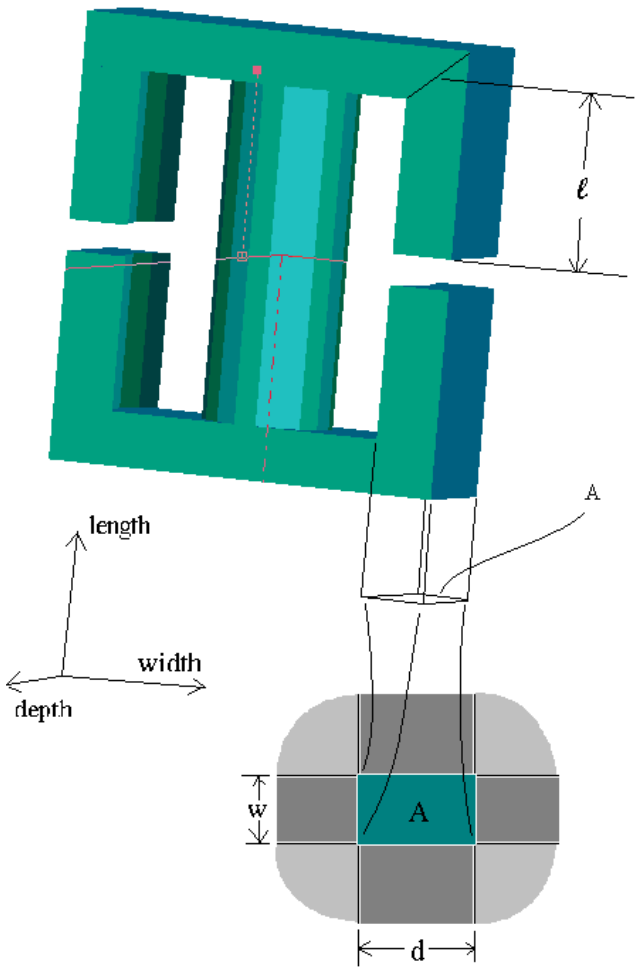

Figure 9: Dimensions for reluctance calculations.

Both of these reluctances are missing a length in their denominators since, as stated above, they are reluctances per unit core depth. We can also represent the fringing reluctance for flux coming from the sides of the transformer leg with dimension d in Figure 9 by the same formula as the flux coming from the sides with dimension w. In total, then, the fringing flux coming from all sides of a transformer leg with perimeter $p = 2(d+w)$ is

$$\Re_{faces} = \frac{\pi}{p \cdot \mu_0 \left(1 + \ln \frac{\pi l}{2 l_{gap}} \right)} \tag{3}$$

This reluctance will be referred to as the reluctance of flux paths emanating from the faces of the leg, or as the "face reluctance," in order to distinguish it from another type of reluctance introduced in the next paragraph.

Thus far we have accounted for all of the fringing flux passing through the darkly shaded regions outside the rectangle in the bottom of Figure 9. However, the two-dimensional, translationally symmetric model to which the formulas in [7] apply precludes the calculation of an effective reluctance for flux going though the lightly shaded regions of Figure 9, which we will refer to as the corner fringing flux; the reluctance of its path is then the "corner reluctance." As no reliable estimate of the reluctance of these corner paths could be found in the literature, we chose to empirically estimate the corner reluctance. In order to do so, we modeled a simple rectangular inductor like that shown in Figure 10, with an air gap in one leg.[1] Through FEA simulation, we found the total reluctance of this inductor. As demonstrated above, we can calculate the total core reluctance, the reluctance of the path directly across the gap, and the reluctance of the non-corner fringing paths. By plugging these values into the total reluctance formula

$$\Re_{total} = \Re_{core} + \Re_{gap} \left\| \Re_{faces} \right\| \Re_{corners}$$

we can numerical determine the corner reluctance for this simplified case. After considering several other formulations, we concluded that the corner reluctance should have the form

$$\Re_{corners} \approx \frac{1}{\mu_0 k l}, \tag{4}$$

where k is some constant quantity. From the above simulation, k was calculated to be about 1.23.

[1] Actually the simple rectangular core was surrounded on the three non-gapped sides by a material of extremely low permeability to ensure that all flux would take some path from the top of the gapped leg to the bottom, rather than leaking through the window or around the non-core side of the winding. This simplified the formula for total R.

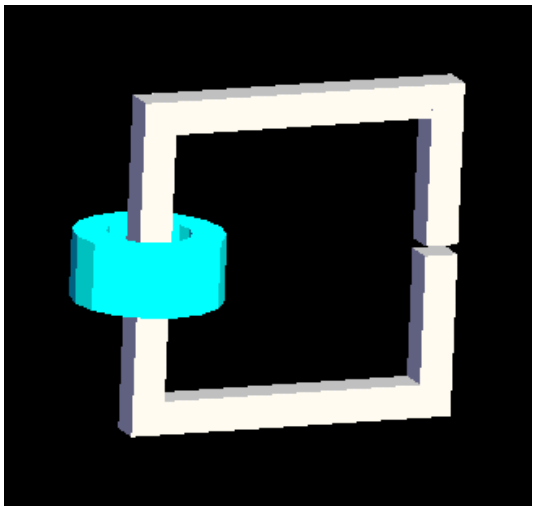

Figure 10: A simplified core for use in estimation of corner fringing.

The final flux path for which we have not yet calculated a reluctance is the path through the winding window. Assuming that the flux does not spread out significantly when passing through the window, the reluctance for this path is

$$\Re_{window} = \frac{h}{\mu_0 w_w d}. \tag{5}$$

The window width w_w and height h are shown in Figure 11, and depth d is as defined in Figure 9. Neglecting the fringing of the flux leakage through the window turns out to be a valid assumption because with or without fringing, the reluctance of the path through the window is very high compared to the other reluctances in the model. A relatively high reluctance in an alternative path aligned in parallel with several paths of lower reluctance means that little flux will flow through the high reluctance path. Therefore the accuracy of the calculation of the window reluctance is not crucial and the simple formula appearing above is sufficient.

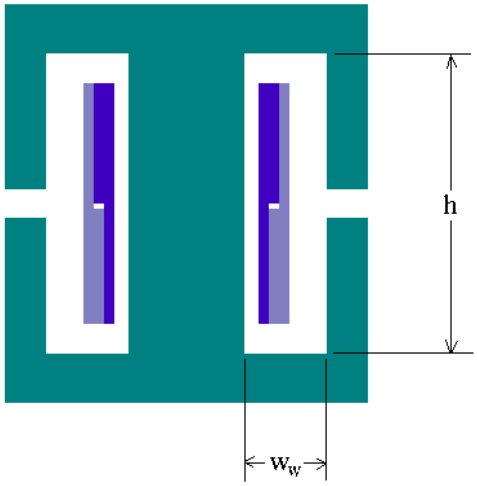

Figure 11: The winding window dimensions.

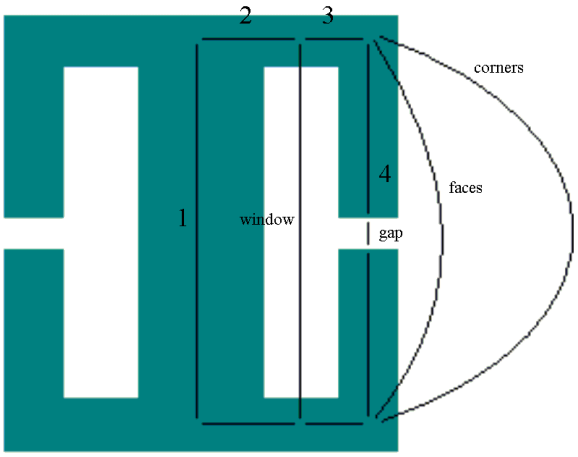

Figure 12: Flux path definitions in the 3D outer gapped transformer.

Combining all these flux paths, we arrive at an expression for the total reluctance of the three-dimensional transformer core with gapped outer legs. The relationship of the various paths is shown in Figure 12. Combining them appropriately, we have

$$\Re_{total,3D} = \Re_1 + \tfrac{1}{2}\left(2\cdot\Re_2 + \Re_{window} \,\|\, \left(2\cdot\Re_3 + \left(2\cdot\Re_4 + \Re_{gap}\right) \,\|\, \Re_{faces} \,\|\, \Re_{corners}\right)\right) \tag{6}$$

where the subscripts refer to the paths defined in Figure 12. This reluctance can then be used to generate the equal reluctance and extended path models. The various numbered reluctances are all easily calculable from transformer geometry based on equation (1). In measuring lengths of transformer legs, it is reasonable (though not exact) to assume that the flux travels through the middle of each leg. An exception to this occurs in the case of the connections of the top and bottom legs to the center post. Flux actually travels near the edges of the center post, so it is more accurate to measure the lengths of the top and bottom legs starting at the outer edge of the center post. This also avoids a problem that arises in the 2D models involving taking the natural logarithm of zero.

It is worth noting that for all 2D models, the reluctance $\Re_1$ of the center post is the same as for the 3D model, so we do not need to explicitly account for it in either. This is the case because we are modeling transformers with round center posts. In the case of a transformer with a differently shaped (e.g. rectangular) center post, it would be fairly accurate to simply give the center post the same cross-sectional area in the 2D model as in the 3D. However, in the case of a gapped, rectangular center post, fringing would differ between the 2D and 3D models since the 2D center post is always round and would therefore not have any corner flux paths. One could account for this by using the reluctance formulas above for face and corner paths to determine the radius that gives a cylindrical center post the same reluctance as a rectangular post of given dimensions; this paper does not address the issue of center post shape beyond this suggestion.

In transformers with no air gap, there is no fringing, so calculation of the reluctance of the 3D model is much less complicated. This is also the case for transformers with a gap only in the center post, since, as noted in the preceding paragraph, the reluctance of the center post is always the same between a 3D model and the corresponding axisymmetric 2D models. It is helpful to include the reluctance of the path through the winding window in our calculation of the total reluctance. The window path is envisioned as leaving the top leg halfway from the inner to the outer leg and re-entering the core in a similar location in the bottom leg, as shown in previously in Figure 13. The reluctance of the window path, again ignoring the small contribution of fringing effects, is

$$\Re_{window} = \frac{h}{\mu_0 w_w d}$$

just as in equation (5) for transformers with a gapped outer leg. The other necessary reluctances are easily determined from the transformer geometry using equation (1). The final equation for the reluctance of a 3D model without a gap in the outer legs is

$$\Re_{total,3D} = \Re_1 + \tfrac{1}{2}\left(2\Re_2 + \Re_{window} \,\|\, \left(2\Re_3 + \Re_4\right)\right).$$

The four numbered reluctances correspond to the flux paths shown in Figure 13. We are now ready to use the 3D reluctance formulas to create the 2D models.

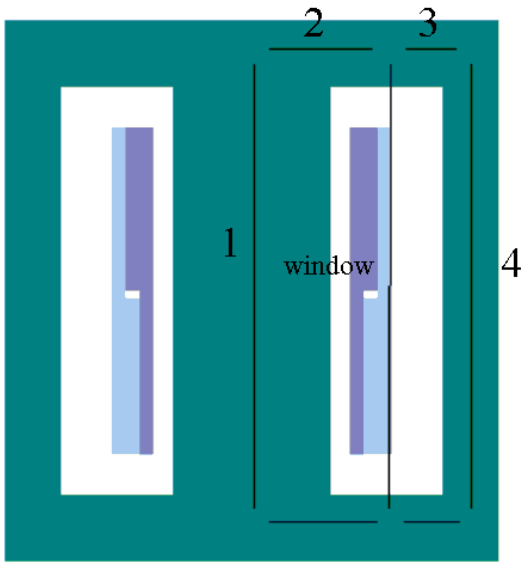

Figure 13: Flux path definitions in the 3D gapless transformer.

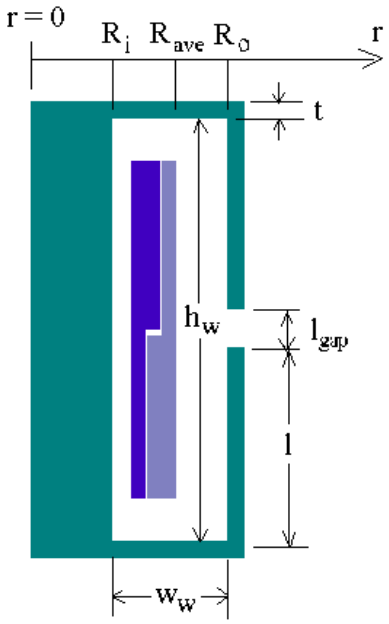

Figure 14: Dimensions of the equal reluctance model.

Drawing the Equal Reluctance Model:

The equal reluctance (ER) model is derived from the model parallel to the transformer core (||) by trimming down the top, bottom, and outer legs. The three trimmed legs have a remaining thickness t, which is determined by giving the ER model the same reluctance as the 3D model calculated above. Therefore we require an expression for the reluctance of the ER model in terms of t, which we can then set equal to $\Re_{total,3D}$ in order to solve for t.

For transformers with an air gap in their outer legs, the ER model also has an air gap, so formulas similar to those used in the calculation of the actual 3D reluctance must be used to account for fringing. In addition, the non-uniform cross-sectional area of the top and bottom legs (due to the model's use of rotational symmetry) means that reluctance must be formulated as an integral, with the usual length quantity is the variable of integration. The cross-sectional area A must be expressed as a function *f* of distance *x* along the *l* axis, so that the general equation for the reluctance of a transformer section of varying cross-section is

$$\Re = \int_0^l \frac{1}{\mu_0 \mu_R \cdot f(x)} dx .$$

In the case of the top or bottom leg of the ER transformer model, the distance *x* is functionally equivalent to the radius *r* from the axis of symmetry, although the integration does not start at *r* = 0 but rather at R_i as defined in Figure 14. Substituting in specific values from Figure 14, we get that

(7) $$\Re_{top} = \Re_{bottom} = \int_{R_i}^{R_o + t/2} \frac{1}{\mu_0 \mu_R \cdot t \cdot 2\pi \cdot r} dr = \frac{\ln \dfrac{R_o + t/2}{R_i}}{\mu_0 \mu_R \cdot 2\pi \cdot t}.$$

For the outer leg the usual formula for reluctance is still valid, although the rotational symmetry of the model must again be taken into account when calculating the cross-sectional area. The reluctance of the outer leg, using the dimensions in Figure 14 and excluding the air gap, is then:

(8) $$\Re_{outer} = \frac{2l + t}{\mu_0 \mu_R \cdot 2\pi \cdot \left(R_0 + t/2\right) \cdot t}.$$

The reluctance of the path directly across the gap is

(9) $$\Re_{gap} = \frac{l_{gap}}{\mu_0 \cdot 2\pi \cdot \left(R_0 + t/2\right) \cdot t}$$

and in parallel with this path there is a fringing path whose reluctance can be calculated using equation (3), which gives the fringing reluctance as a function of perimeter. In this case the perimeter is rather extensive due to the rotation of the outer leg around the central axis. The total perimeter of the cylindrical leg facing the gap is

$$p = 2\pi \cdot Ro + 2\pi \cdot (Ro + t) = 2 \cdot \left(2\pi \cdot \left(R_o + t/2\right)\right),$$

and substituting this into equation (3) gives

$$\Re_{fringe} = \frac{1}{\mu_0 \cdot 2 \cdot \left(2R_0 + t\right) \cdot \left(1 + \ln \dfrac{\pi \cdot l}{2 l_{gap}}\right)}.$$

We then have the total reluctance of the ER model as a function of t

(10) $$\Re_{total,ER} = \Re_1 + 2 \cdot \Re_{top} + \Re_{outer} + \Re_{gap} \| \Re_{fringe}$$

as illustrated in Figure 15. Finally, we set this equal to $\Re_{total,3D}$ in order to solve for t, and we have our ER model. [2]

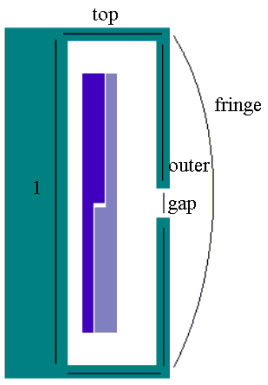

Figure 15: Flux paths in the equal reluctance model.

[2] Solving for t algebraically is a daunting task, if not impossible. Solving numerically is recommended.

For transformers with no air gap in their outer legs, the process of finding the thickness t is much simpler, since no gap means no fringing. However, it is useful to account for the flux path through the window in this case. We were able to neglect the window flux in the outer gapped case because relative to other non-core fluxes, the window flux was small. Since there are no other non-core fluxes in the gapless case, we include the window reluctance, which from Figure 14 is

$$\Re_{window} = \frac{h_w}{\mu_0 \cdot 2\pi \cdot R_{ave} \cdot w_w}.$$

The window flux path can be approximated as in parallel with the path through the top, outer, and bottom legs the top and bottom legs are relatively short and the windings are concentrated in the centermost part of the window. In a transformer with different geometry it might be more accurate to treat the window flux as leaving the top leg halfway between the inner and outer legs, as shown in Figure 13.

We can use the same expressions for $\Re_{top}$, $\Re_{bottom}$, and $\Re_{outer}$ as were used in the gapped case since none of them involved the gap effects. Hence we have the following expression for the total reluctance of the ER model of a transformer with no outer gap:

$$\Re_{total,ER} = \Re_1 + \Re_{window} \left\| \left(2 \cdot \Re_{top} + \Re_{outer} \right) \right.$$

Once again, setting this equal to $\Re_{total,3D}$ allows us to solve for t.

Drawing the Extended Path Model:

The extended path (XP) model is created by adding an extended flux return path to the model of the section perpendicular to the transformer core (T). The first step in drawing the extended flux path is determining how far away it should be from the windings in order to accurately simulate the 3D situation. This determination does not need to be precise, as the exact distance does not have a large effect on the results of the simulation, but it should be in the right ballpark. The two dimensions to be determined are the height and width of the window framed by the extended path and the transformer's center post. We choose the height of the window so that the distance *e* from the top leg of the extended path to the center of the winding region is the same as the distance on the 3D model from the center of the top leg to the center of the winding region in the plane perpendicular to the core. Likewise, we choose the width of the window so that the distance *d* from the center of the winding region to the outer leg of the extended path is the same as the distance on the 3D model from the center of an outer leg to the center of the winding region in the plane perpendicular to the core. Figure 16 is a diagram of the geometrical equivalence used to estimate *d* and *e*.

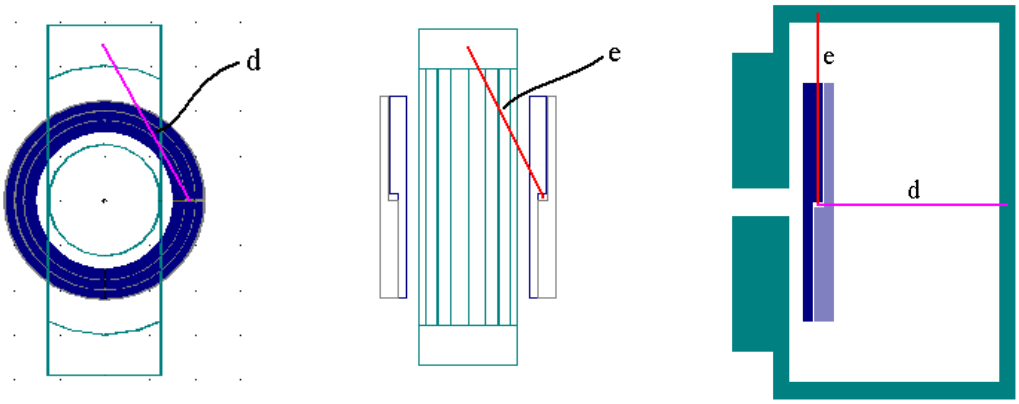

Figure 16: Finding the dimensions of the extended path.

Once *d* and *e* have been determined, the reluctance of the XP model is set equal to the calculated reluctance of the 3D model in a manner similar to that used in the ER model. Once again we will use the thickness parameter t to set the 2D model's reluctance. The primary difference is that we do include the effects of the much larger winding window by representing the leakage through the window as a path with reluctance $\Re_{window}$ that jumps from the middle of the top leg to the middle of the bottom leg. As with all other models, the geometry and reluctance of the center post are the same in the 2D model as in the 3D model and do not need to be accounted for explicitly. A diagram of the XP model with illustrations of the dimensions used to calculate its reluctance is shown in Figure 17. The reluctance of the short legs running from the center post to the top and bottom legs is

$$\Re_{nearlegs} = \frac{2(e-c)}{\mu_0 \mu_R \cdot 2\pi \cdot \left(R_i - t/2\right) \cdot t}. \tag{11}$$

The reluctance of the top and bottom legs once again requires an integral over the radius r from R_i to R_o, resulting in the reluctance

$$\Re_{top} = \Re_{bottom} = \int_{R_i}^{R_w+d} \frac{1}{\mu_0 \mu_R \cdot t \cdot 2\pi \cdot r} dr = \frac{\ln \dfrac{R_w + d}{R_i}}{\mu_0 \mu_R \cdot 2\pi \cdot t}. \tag{12}$$

The XP model never includes an air gap in the extended flux return path because the addition of an air gap far from the axis of symmetry creates a gap region with an unrealistically large perimeter. As we saw before, the perimeter of the cross-section of a core leg is a principal factor in the reluctance of any air gaps in that leg, so an unrealistically large perimeter leads to an unrealistic gap reluctance. Also, the absence of a gap does not have a major effect on the model since at the increased distance from the wires the effects of such a gap are less significant (except for its effect on overall reluctance, which is accounted for by the path thickness). The absence of an air gap makes the reluctance of the outer leg easy to calculate:

$$\Re_{outer} = \frac{2e}{\mu_0 \mu_R \cdot 2\pi \cdot \left(R_w + d\right) \cdot t}. \tag{13}$$

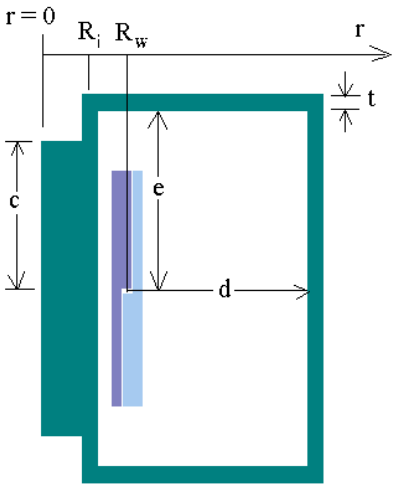

Figure 17: The dimensions of the extended path model.

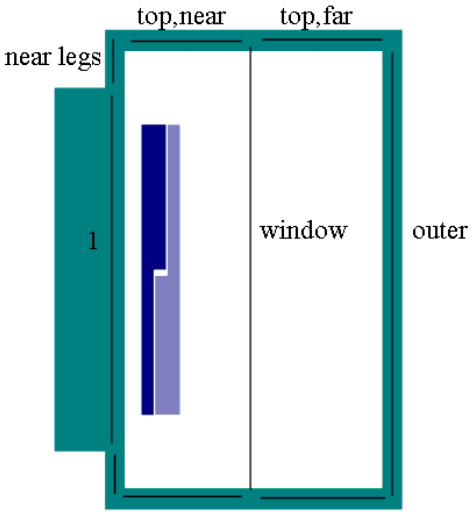

Figure 18: Flux paths in the extended path model.

The final flux path to account for in the XP model is the path through the winding window. From the geometry in Figure 17, and remembering the cylindrical symmetry, the window reluctance is

$$\Re_{window} = \frac{2e}{\mu_0 \cdot \pi \cdot \left(\left(d + R_w\right) + R_i\right) \cdot \left(d + R_w - R_i\right)}. \tag{14}$$

We have taken advantage of the fact that t<<d and t<<e in order to simplify the above formula. The window flux is represented as a path through the middle of the window, as shown in Figure 18. Thus we will need to split up the integral for the top and bottom leg reluctances into two parts: one integral from R_i to the middle of the window at $(R_w+d+R_i)/2$, and the other from the middle of the window to the outer leg at R_w+d. We define these two integrals as $\Re_{top,near}$ and $\Re_{top,far}$, respectively, based on their distances from the center post. The integrand in both is the same as the integrand of $\Re_{top}$ above.

Using the above definitions, we can now write

$$\Re_{total,XP} = \Re_1 + \Re_{nearlegs} + 2 \cdot \Re_{top,near} + \Re_{window} \left\| \left(2 \cdot \Re_{top,far} + \Re_{outer}\right) \right. \tag{15}$$

as dictated by the flux path diagram in Figure 18. Finally we set this equal to $\Re_{total,3D}$, and solving for t as usual provides the final parameter needed to draw the XP model. Since the XP model never includes an air gap in its outer leg, the same formula for $\Re_{total,XP}$ applies to transformers both with and without an air gap in their outer leg.

III. Example calculations and results

This section contains sample calculations of the various quantities described above for the specific case of the specific case of the transformer with gaps in all legs with dimensions shown in Figure 19. Note that the calculations would be exactly the same if they were done for a transformer with gaps only in the outer legs. The only difference between the two models is the presence of absence of a gap in the center post. (You can literally create an outer gapped 2D model by filling in the center gap in the appropriate all-gapped 2D model.) The same its true of the two transformers without gaps in the outer legs: the gapless transformer is identical except for the center post to the center-gapped transformer.

Following the sample calculations are the results from each model for all of the transformer configurations studied. The results from the various models are compared, using the accurate 3D model as a baseline.

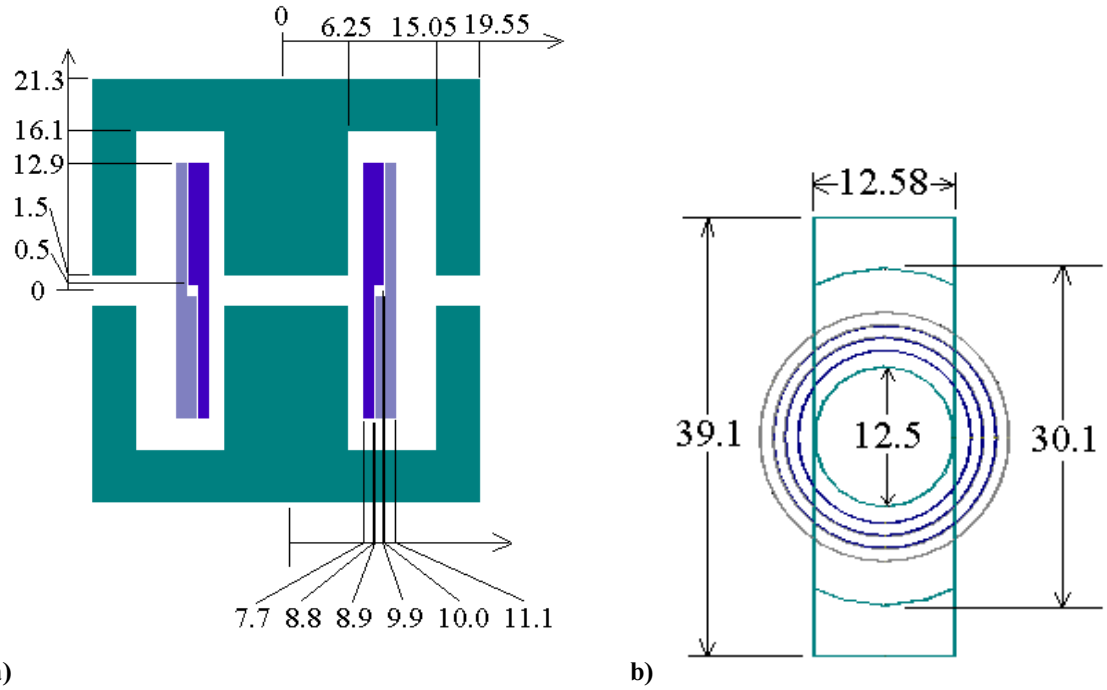

a) b)

Figure 18: Dimensions of the example transformer in mm. (The dimensions on the diagram on the left are in mm from the center of the transformer core.) a) Front view. b) Top view.

An Example Using a Transformer with Gaps in All Legs:

The first step in creating the 2D models is to find the reluctance of the actual 3D transformer. Since there are gaps in the outer legs, we use equation (6):

$$\Re_{total,3D} = \Re_1 + \tfrac{1}{2}\left(2\cdot\Re_2 + \Re_{window} \left\| \left(2\cdot\Re_3 + \left(2\cdot\Re_4 + \Re_{gap}\right) \right\| \Re_{faces} \right\| \Re_{corners}\right)\right)$$

We do not need to calculate $\Re_1$ since it will be the same in the 2D models and will cancel out. Using equation (1) and the geometry in Figure 18 we find

$$\Re 2 = \frac{7.525}{\mu_0\mu_R 12.58\cdot 5.2} = 4.58\cdot 10^4 \text{ H}^{-1},$$

$$\Re 3 = \frac{2\cdot 6.65}{\mu_0\mu_R 12.58\cdot 5.2} = 8.09\cdot 10^4 \text{ H}^{-1},$$

and

$$\Re 4 = \frac{17.2}{\mu_0\mu_R 62.276} = 2.20\cdot 10^5 \text{ H}^{-1}.$$

Referring to equations (2) and (5), we get

$$\Re_{gap} = \frac{3}{\mu_0 62.276} = 3.83\cdot 10^7 \text{ H}^{-1}$$

and

$$\Re_{window} = \frac{2\cdot 16.1}{\mu_0 8.8\cdot 12.58} = 2.31\cdot 10^8 \text{ H}^{-1}.$$

The relative permeability μ_0 used in the above cases was 2000, as is true of all models simulated. Since the *l* is not the same for all four faces of the outer leg, we must split $\Re_{faces}$ into a path representing the fringing from the inner face and another representing the fringing from the three other faces. The two paths run parallel: $\Re_{faces} = \Re_{innerface} \| \Re_{otherfaces}$. Calculated from equation (3), these two reluctances are

$$\Re_{innerface} = \frac{\pi}{12.58\cdot\mu_0\left(1+\ln\frac{\pi\cdot 14.6}{2\cdot 3}\right)} = 6.55\cdot 10^7 \text{ H}^{-1}$$

and

$$\Re_{otherfaces} = \frac{\pi}{\left(12.58+2\cdot 4.5\right)\cdot\mu_0\left(1+\ln\frac{\pi\cdot 17.2}{2\cdot 3}\right)} = 3.62\cdot 10^7 \text{ H}^{-1}.$$

Therefore,

$$\Re_{faces} = 2.33\cdot 10^7 \text{ H}^{-1}.$$

And finally,

$$\Re_{corners} = \frac{1}{\mu_0 1.23\cdot 16.1} = 4.07\cdot 10^7 \text{H}^{-1}.$$

All of the preceding calculations used μ_0=1.2566*10^{-9} H/m, an adjustment for the fact that all dimensions are in millimeters. The final reluctance of the 3D transformer comes to

$$\Re_{total,3D} = 5.24\cdot 10^6 + \Re_1.$$

Next we will create the ER model. The only parameter we need for that is the thickness *t* of the top, bottom, and outer legs. To find *t*, we set an expression in terms of *t*

for the reluctance of the ER model equal to the total 3D reluctance. According to equation (10), the total ER model reluctance is

$$\Re_{total,ER} = \Re_1 + 2 \cdot \Re_{top} + \Re_{outer} + \Re_{gap} \| \Re_{fringe} .$$

Substituting the values from Figure 18 into equations (3), (7), (8), and (9), and subsequently plugging the resulting formulas into the above equation (without subjecting the reader to the process this time) yields a long, complicated equation for $\Re_{total,ER}(t) = \Re_1 + \Re_{rest}(t)$. Setting this equal to $\Re_{total,3D} = 5.24 \cdot 10^6 + \Re_1$ and solving for *t* gives the result *t*=1.8950 cm. This solution was obtained numerically using the Solver function of a Texas-Instruments TI-85 calculator.

The next step is to create the XP model. To do that, we first need to find the parameters *d* and *e* that define the window size. From Figures 16, we calculate that $d = \sqrt{9.4^2 + 17.3^2} = 19.69$ cm, and $e = \sqrt{5.275^2 + 18.7^2} = 19.43$ cm. We can then use these values in equations (11), (12), (13), and (14) to come up with a group of equations to substitute into equation (15), giving an expression for $\Re_{total,XP}(t) = \Re_1 + \Re_{rest}(t)$. Just as in the ER model, we set this equal to $\Re_{total,3D}$ and solve numerically for *t*. The resulting thickness is *t*=0.0617 cm. It is reasonable that the thickness of the XP model is much less than the thickness of the ER model since the ER model contains an air gap to increase its reluctance whereas the XP model's reluctance can only be decreased by lowering the cross-sectional area of the extended path. Now we have all three parameters (*d*, *e*, and *t*) used in the XP model and are ready to draw it.

Once the ER and XP models have been simulated by FEA, we are ready to combine the results to form the ERXP weighted average model. The weighting factor *w* for our example transformer can be found from the diagram in Figure 8 to be *w*=26.82/(26.82+23.38)=0.534. In order to calculate, for example, the magnetic energy in the windings of the transformer with gaps in all legs under magnetizing excitation using the ERXP model, we first run the ER and XP simulation and obtain their values of the energy in the windings. The ER model gives 1.270*10-8 J, and the XP model gives 1.052*10-8 J, so the ERXP model's solution is *w**1.052*10-8+(1-*w*)*1.270*10-8=1.154*10-8 J. The ||T weighted average model can be obtained in the same manner. The T section represents the same plane as the XP model and the || section represents the same plane as the ER model, so they are weighted accordingly.

Results and Comparison of Models: [3]

The other three transformers modeled in this study have the same dimensions as the one in Figure 18 with the exception of varying gap locations. In all cases the gap is three millimeters long and placed in the center of the leg in which it lies. What follows is an analysis of the simulation results for all four transformers under both magnetizing and leakage current. As noted previously, the total magnetic energy of the system and the magnetic energy in the windings are the quantities used to judge the simulations.

Figure 19 is a graphical representation of the results of the four individual 2D

[3] All 2D simulations were run on Ansoft's Maxwell 2D Field Simulator Version 7 software, a FEA tool for electromagnetic systems. All 3D simulations used the same company's Maxwell 3D Field Simulator Version 5.

models and the two combined 2D models for a center-gapped transformer. In addition, the result for the 3D model is shown with darker shading on the far left of each plot for comparison. The top two charts are of models of the transformer under magnetizing excitation, and the bottom two charts are of models of the transformer under leakage excitation. The two charts on the left represent the results for the total magnetic energy of the system, and the two charts on the right show the results for the magnetic energy in the windings.

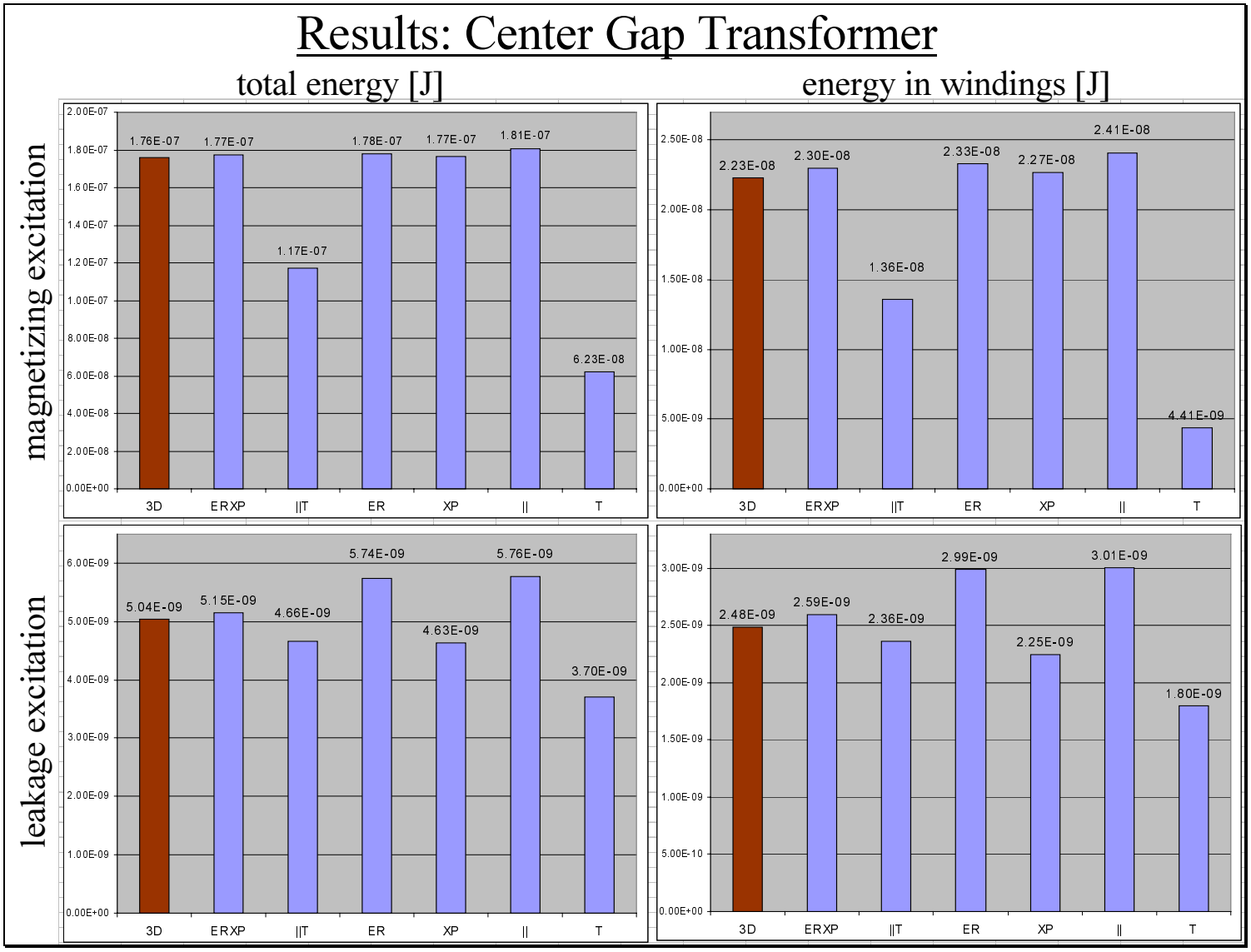

Figure 19: Results for the center gapped transformer.

It is clear from Figure 19 that the ERXP model always returns a value quite close to the 3D value. In certain cases one or two other models come closer to the 3D model than the ERXP, but in other cases those models are significantly off. The ERXP model is the most consistently accurate.

Figures 20, 21, and 22 show similar chart groups for the outer gapped transformer, the transformer with a gap in all legs, and the gapless transformer. Inspection of all the charts demonstrates that the ERXP is in general the best model. The energy in the windings of the gapless transformer under magnetizing excitation is the only value the ERXP fails to calculate within a few percentage points of the 3D model. This case will be discussed more extensively below.

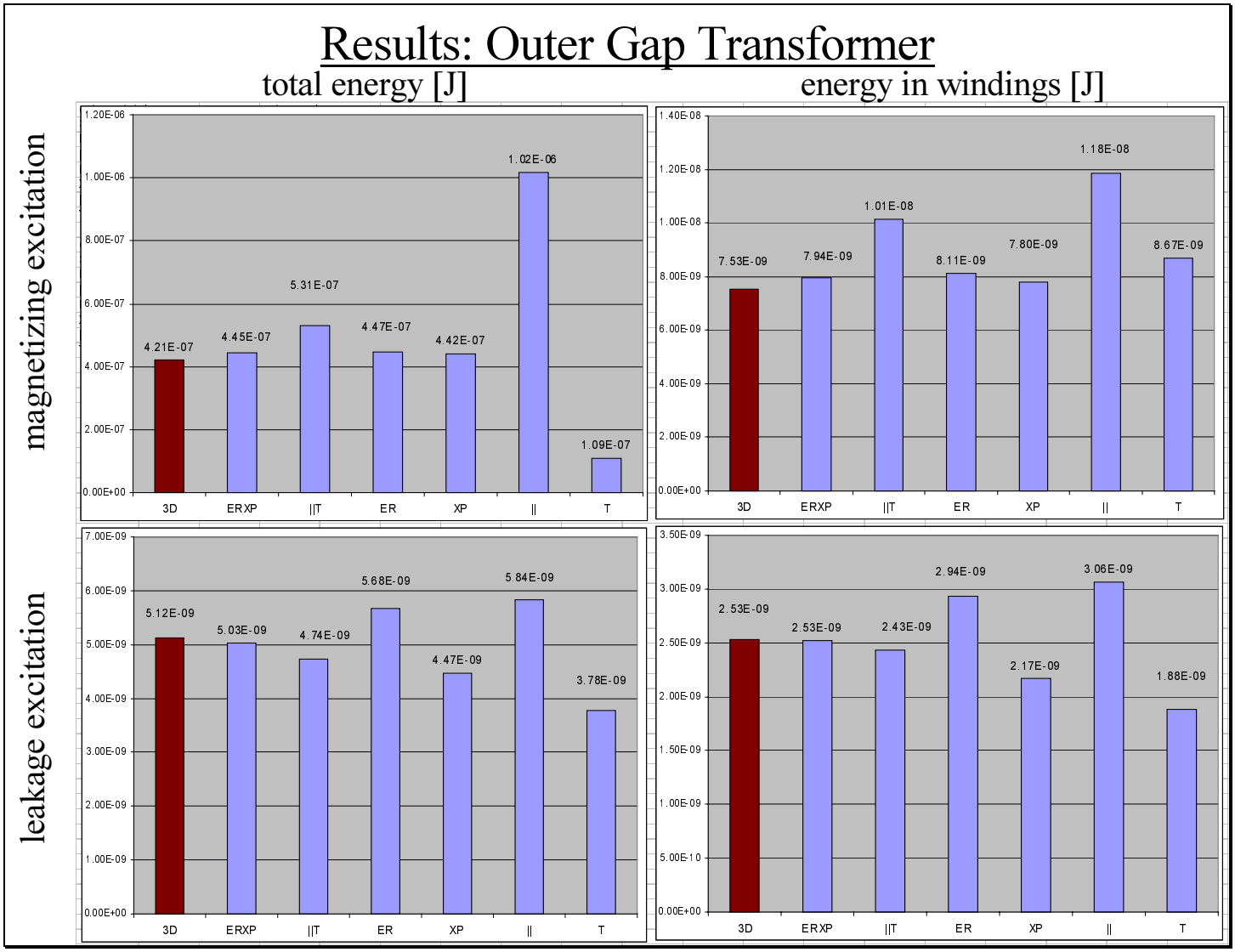

Figure 20: Results for the outer gapped transformer.

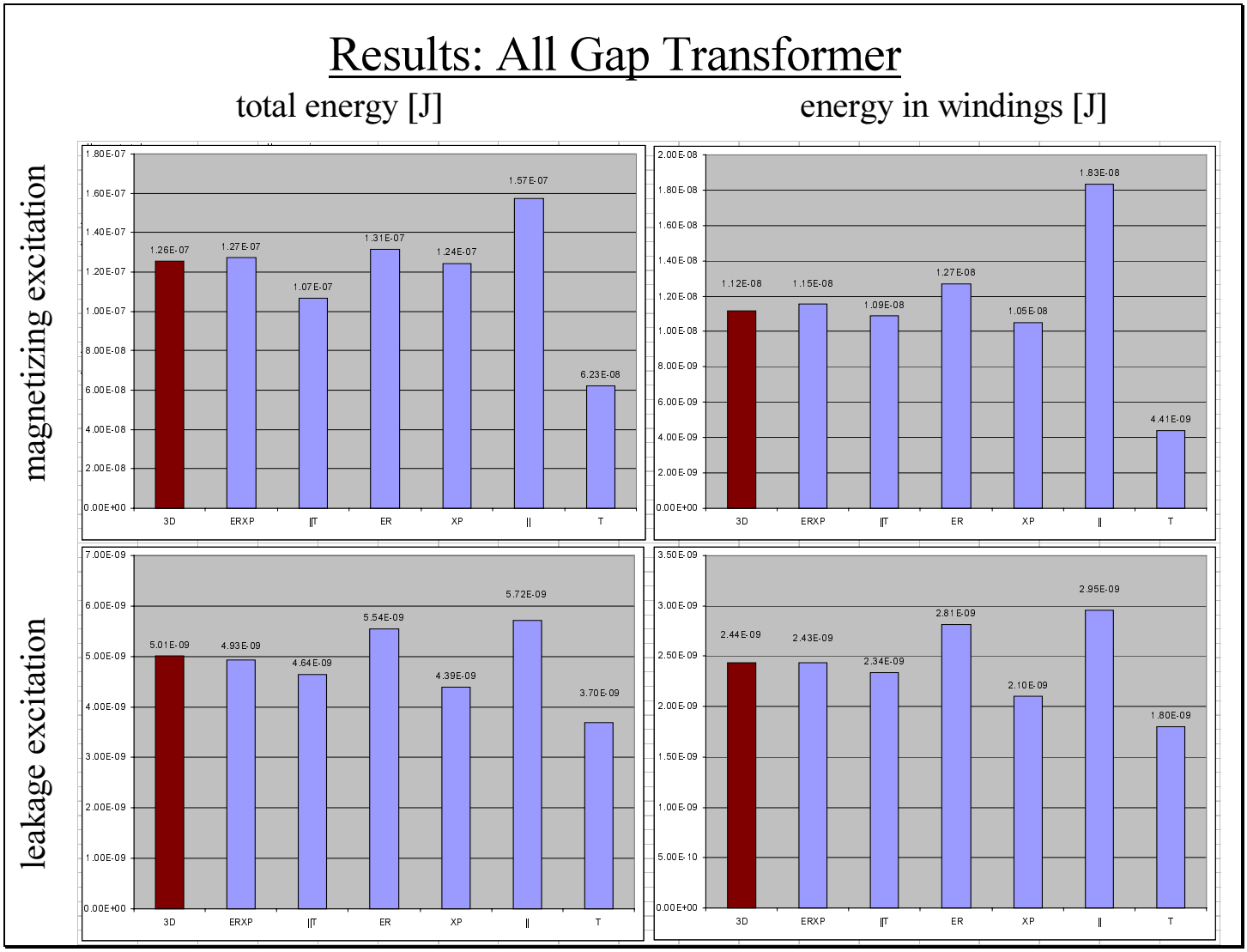

Figure 21: Results for the transformer with gaps in all legs.

Figure 22: Results for the gapless transformer.

Another useful way to view the results is by comparing two different modeling methods across all the situations modeled. Figures 23, 24, and 25 compare the new ERXP model to the three models that have been proposed by other authors: ||, ER, and ||T. In each case the percent errors (relative to the 3D model) of the two models being compared are graphed side by side for each of the 16 situations simulated. Note that the vertical scale varies from chart to chart.

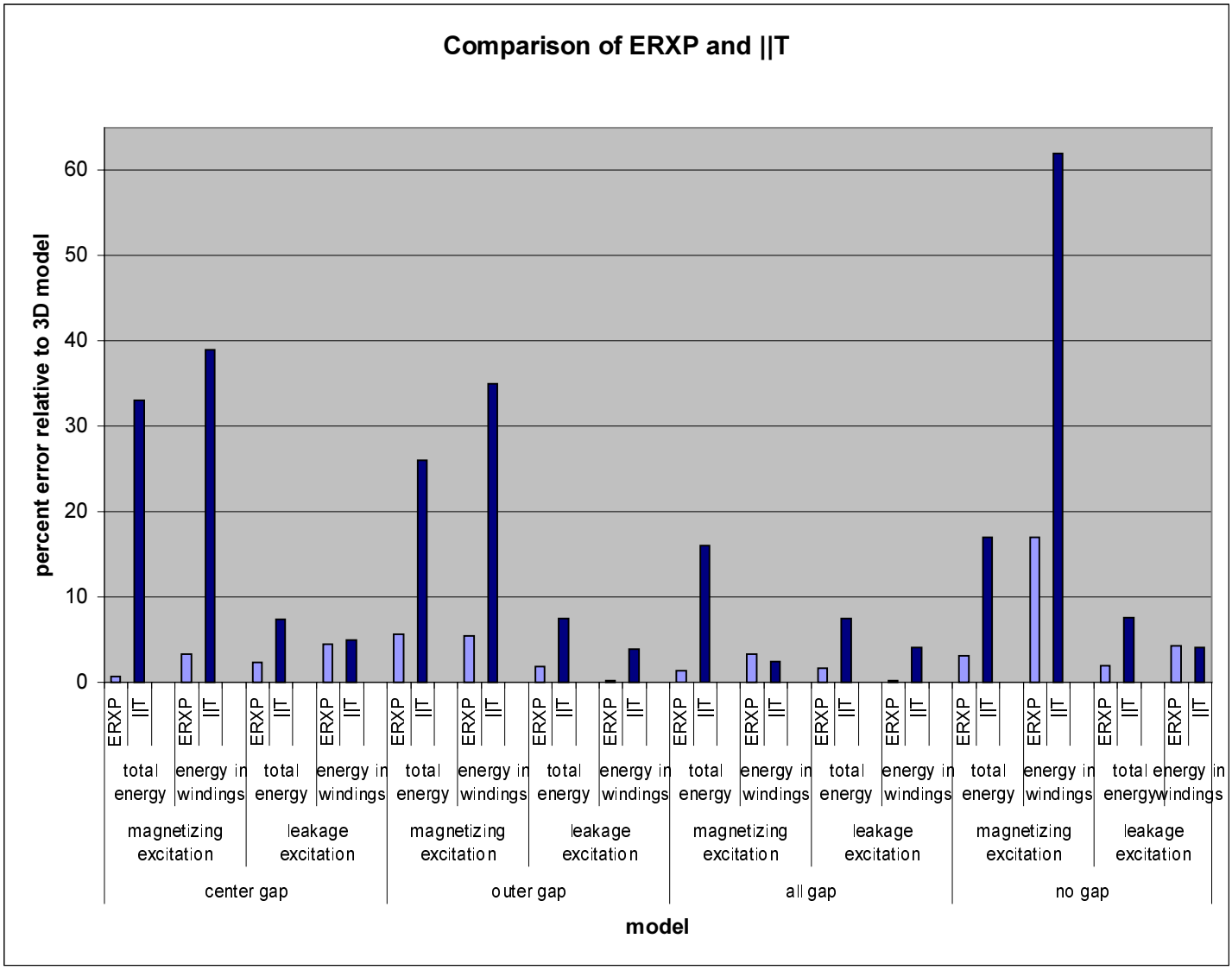

Figure 23: Comparison of the results from the ERXP model and the ||T model.

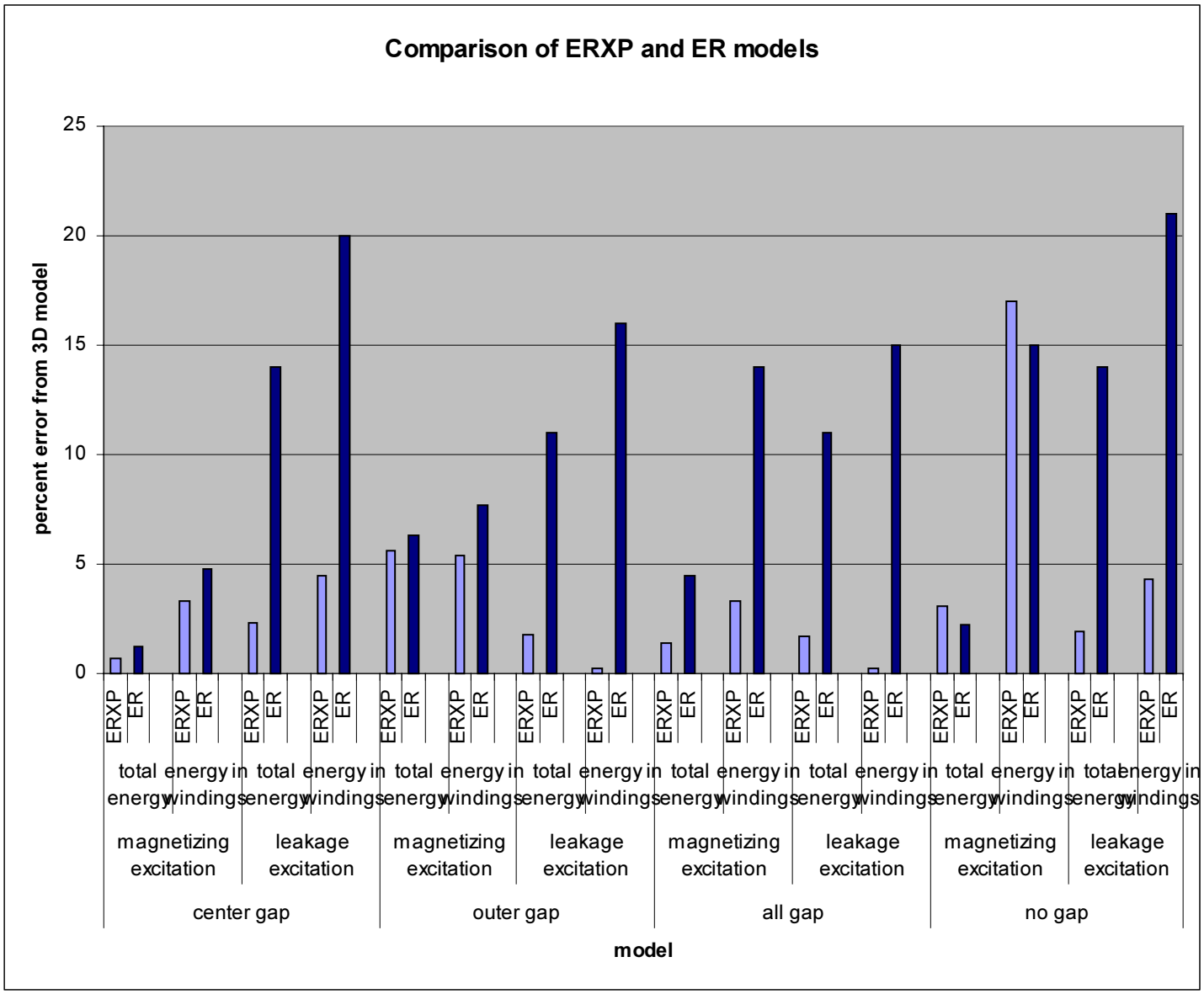

Figure 24: Comparison of the results from the ERXP model and the ER model alone.

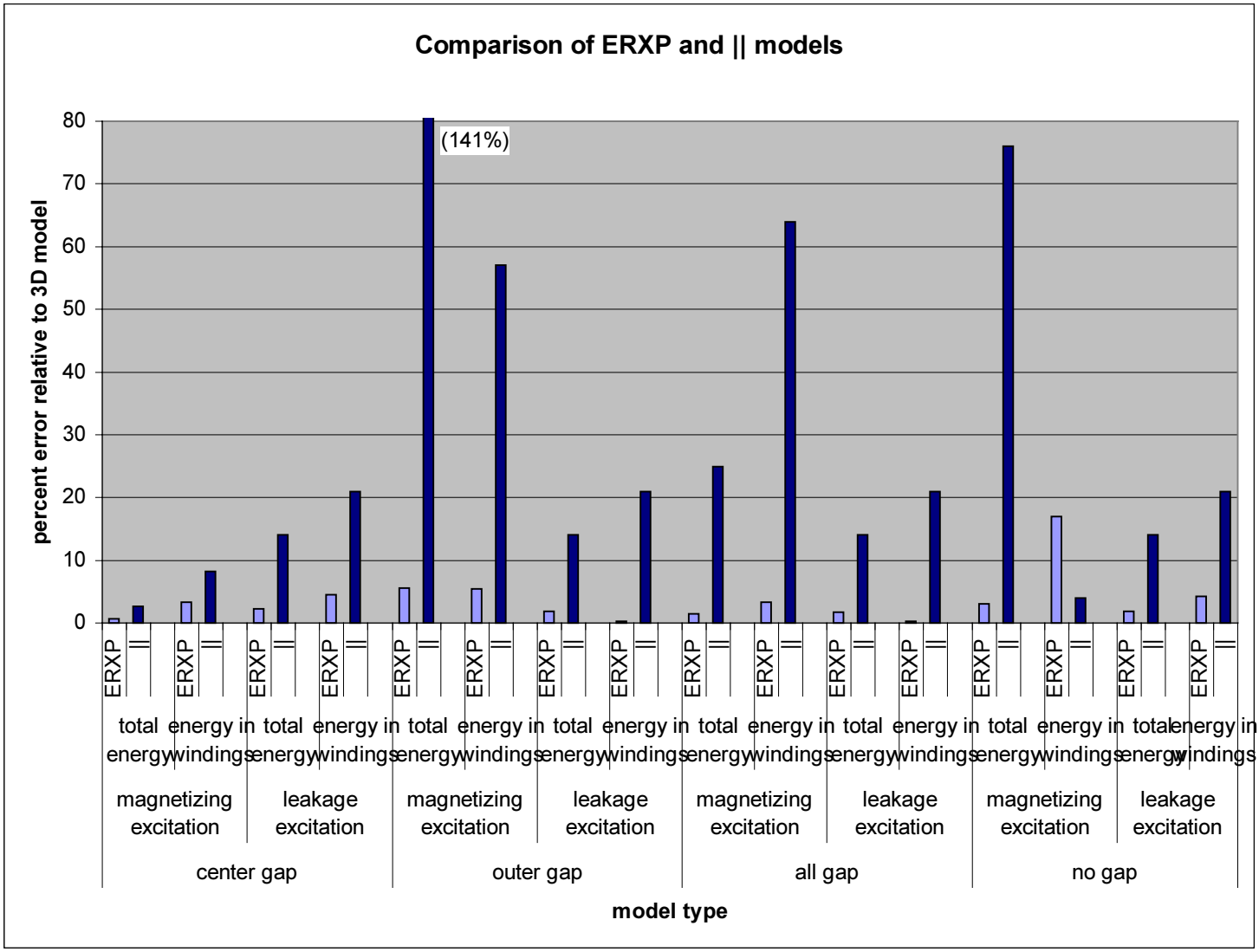

Figure 25: Comparison of the results from the ERXP model and the || model.

The three preceding charts further show the ERXP model to be the most consistently accurate. However, it is apparent from each that the ERXP model falls short of its usual accuracy in the case of the energy in the windings of the gapless transformer under magnetizing excitation. In this case it is still much better than the ||T model and comparable to the ER model. The || model achieves much better accuracy, but this appears to be somewhat of a fluke for two reasons. To begin with, when taking all 16 situations into account, the || model is the least accurate of the four under consideration, and it is the second least accurate of the six existing models, better only than the dubious T model. However, it is certainly possible that in the unique situation of gapless transformers with magnetizing current, the || model works best. However, the 76% error in the || model's prediction of the total energy in this situation corroborates the theory that it will not prove a reliable predictor of winding energy in most cases, given that winding energy and total energy are two results of the same simulation. Thus, it is reasonable to

conclude that the ERXP model is not significantly inferior to other models even in its worst case.

The question of why the ERXP model is uncharacteristically inaccurate in one specific situation is an interesting one. The most obvious characteristic unique to this situation is that the flux never has to leave the core to complete its circuit around the current carriers. All other cases either contain a gap or are under leakage excitation. (Leakage excitation, i.e. current flowing the opposite direction in each winding, causes flux to travel between the windings, clearly forcing it to leave the core.) In any situation involving flux leaving the core, the effect of the non-core path dominates the calculation of reluctance and of any quantities that depend on reluctance, such as inductance and energy. Therefore, one might guess that the reason for the inaccuracy of the ERXP model in the one case where flux does not have to leave the core is that our modeling of how the flux behaves in the core is inaccurate, and that the existence of non-core flux paths overshadows this inaccuracy in other cases. However, the total magnetic energy, which is much more directly dependant on the reluctance than is the winding energy, is predicted to 3% accuracy by the ERXP model.

In other words, the ERXP model gets the total amount of flux right; it just does not accurately predict is location (or, more specifically, its magnitude in the winding region). To investigate what may have gone wrong, it is interesting to look at some plots of the actual magnitude of the B-field generated from each model. Figures 26a, b, and c show plots of the magnetic energy in the three models of the plane perpendicular to the transformer core. The various shades of gray have the same significance in each model, and the range of values has been chosen to facilitate analysis of the field in the windings. The winding region is outlined in each.

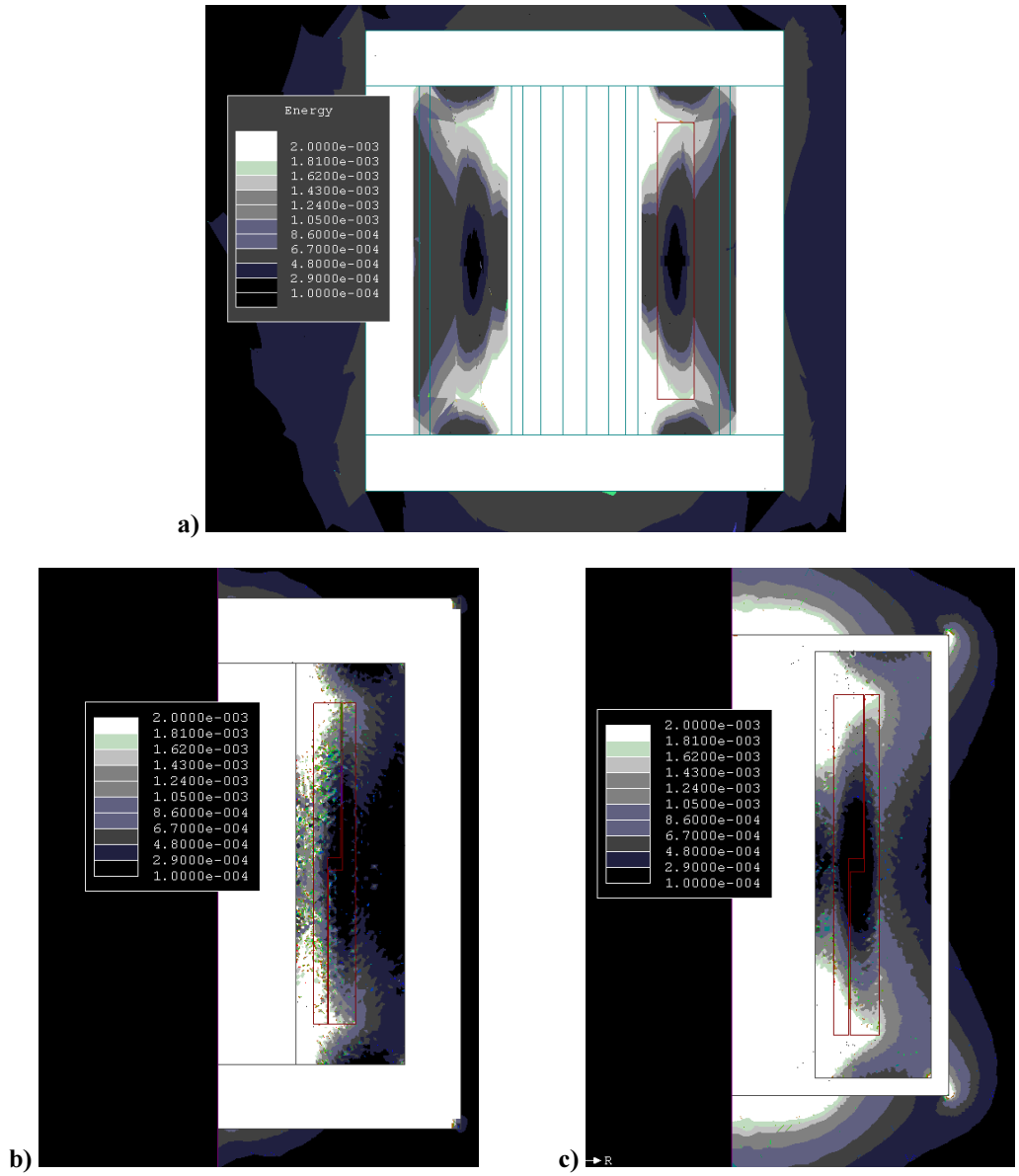

Figure 26: The magnetic energy in Joules for the three models of the plane parallel to the core.

Visual inspection of Figure 26 seems to indicate that the energy in the winding region is more similar to the 3D model in the ER model than in the || model. However, the || model's numerical approximation of the total energy is much closer to that of the 3D model. Both the ER and || models appear to show somewhat less energy in the winding region than the 3D model, but numerically both calculate more energy in the windings than the 3D.

Figures 27a, b, and c show plots of the energy in the plane perpendicular to the core from the three models of that plane. In this case the XP model appears significantly more accurate than the T model. This is indeed the case. The XP model appears to show somewhat less energy in the winding region than the 3D model. However, the XP model has 18% more energy in the windings numerically.

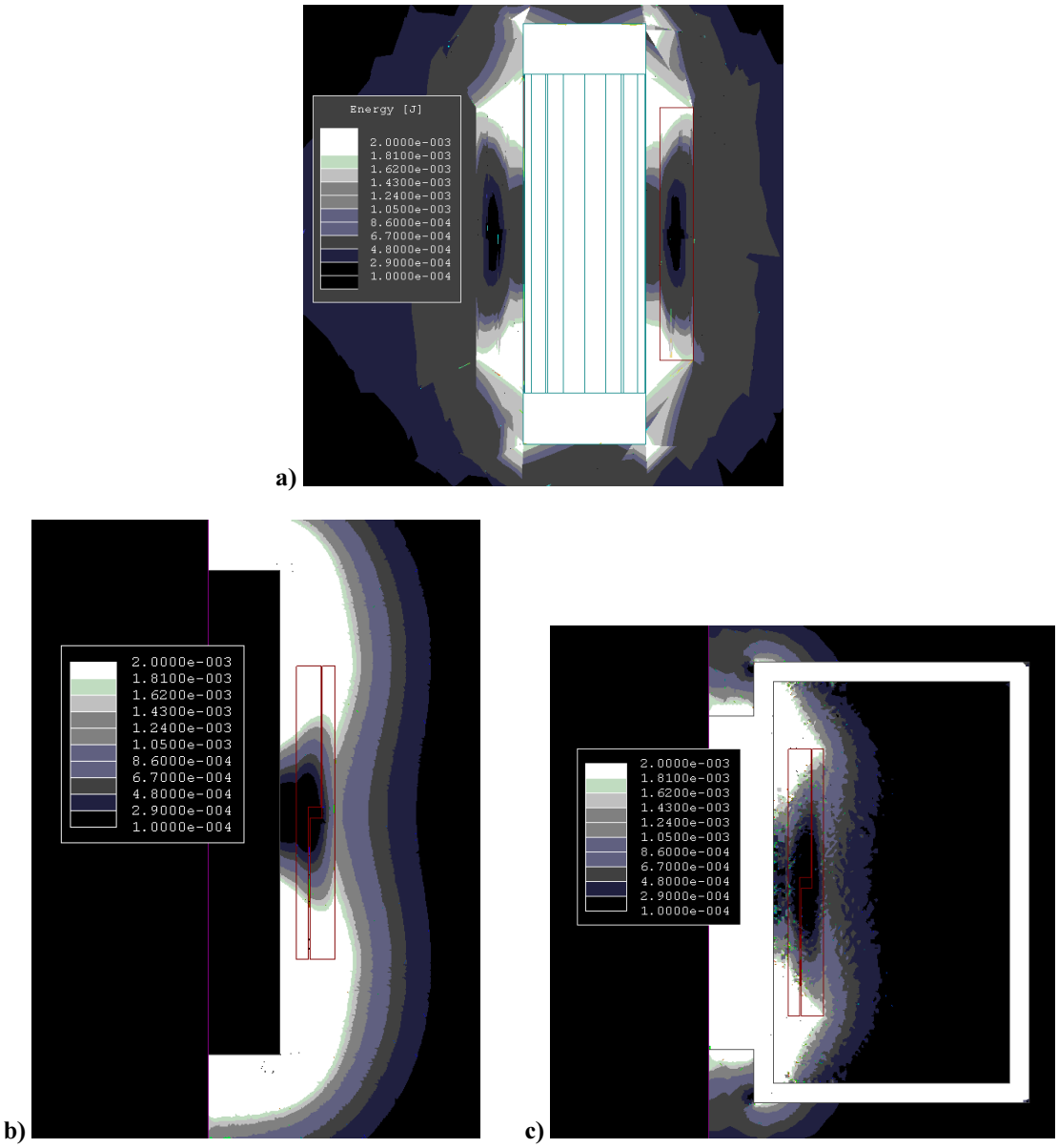

Figure 27: Plots of the magnetic energy in Joules from the three models of the plane perpendicular to the core.

The qualitative conclusions that we have been able to draw from Figures 26 and 27 have not helped explain the increased error of the ERXP model in the case of the energy in the windings of the gapless transformer under magnetizing induction. In fact, both the ER and XP models appear to simulate the energy in their respective planes fairly accurately. The fact that they appear accurate but are off by 15% and 18% is not contradictory, since one would not expect to be able to judge a model precisely by this visual method. In addition, Figure 26b provides more support for the hypothesis that the accuracy of the || model in this case is due largely to chance, since the || model does not appear to be an extremely accurately simulation of the energy distribution compared to the 3D model.

IV. Conclusions

The new ERXP model of E-core transformers is accurate to within 0.2 to 5.6% error in 15 of the 16 cases studied, as compared to the 3D model. It is useful in all four different gap configurations studied under both magnetizing and leakage current, and it accurately predicts both the total magnetic energy and the magnetic energy in the windings. In the gapless transformer under magnetizing excitation, its prediction of the energy in the windings was off by 17%. However, in gapless transformers, the magnetizing current is usually small compared to other currents, so the loss related to this current is very small compared to other sources of loss. Therefore the reduced accuracy of our model in this one case is not detrimental to its usefulness.

In comparison to the other models studied across all situations modeled, the ERXP model is clearly the most generally accurate. In the few cases where some other model is slightly more accurate, both the ERXP and the more accurate model have very low errors. Also, all other models failed to predict certain values within a useful degree of accuracy, while the ERXP did not. It is expected that the ERXP model can be a very useful tool for designers and researchers in the future. Further testing involving simulation of different transformer geometries as well as comparison to physical measurements will hopefully confirm its effectiveness.

V. Acknowledgements

The author would like to thank Charlie Sullivan, the originator of the extended flux return path, for his invaluable help on this project and for the ideas he contributed.

References:

[1] Ohdachi Y, Kawase Y, Tainaka T, and Yamaguchi T, "Load Characteristics Analysis of Coupling Transformers Using 3-D Finite Element Method With Edge Elements", *IEEE Transactions on Magnetics*, vol. 30, pp. 3721-4, 1994.

[2] Kladas A G, Papadopoulos M P, and Tegopoulos J A, " Leakage Flux and Force Calculation on Power Transformer Windings Under Short-Circuit: 2D and 3D Models Based on the Theory of Images and the Finite Element Method Compared to Measurements", *IEEE Transactions on Magnetics*, vol. 30, pp 3487-90, 1994.

[3] Prieto R, Cobos J A, Bataller V, García O, and Uceda J, "Study of Toroidal Transformers by Means of 2D Approaches", *IEEE Power Electronics Specialists Conference (PESC) '97*, vol. 1, pp. 621-6, 1997.

[4] Prieto R, Østergaard L, Cobos J A, and Uceda J, "Axisymmetric Modeling of 3D Magnetic Components", *Proceedings of Applied Power Electronics Conference (APEC) '99*, vol. 1, pp. 213-9, 1999.

[5] Prieto R, Cobos J A, García O, Alou P, and Uceda J, "Model of Integrated Magnetics by Means of 'Double 2D' Finite Element Analysis Techniques", *IEEE Transactions on Magnetics,* pp.598-603, 1999.

[6] Imre T G, Cronje W A, van Wyk J D, and Ferriera J A, "Experimental Validation of Loss Calculations for a Planar Inductor", *IEEE Power Electronics Specialists Conference (PESC) '99*, pp. 586-91, 1999.

[7] Balakrishnan A, Joines W T, and Wilson T G, "Air-Gap Reluctance and Inductance Calculations for Magnetic Circuits Using a Schwarz-Christoffel Transformation", *IEEE Transactions on Power Electronics*, vol. 12, no 4., pp. 654-63, 1997.